Transparent exopolymer particle (TEP) distribution and in situ prokaryotic generation across the deep Mediterranean Sea and nearby North East Atlantic Ocean

Eva Ortega-Retuerta, Ignacio P. Mazuecos, Isabel Reche, Josep M. Gasol, Xosé A. Álvarez-Salgado, Marta Álvarez, María F. Montero, Javier Arístegui

Transparent Exopolymer Particle (TEP) distribution and in situ prokaryotic generation across the deep Mediterranean Sea and nearby North East Atlantic Ocean

Eva Ortega-Retuerta[1, 2*], Ignacio P. Mazuecos[3], Isabel Reche[3, 4], Josep M. Gasol[1, 5], Xosé A. Álvarez-Salgado[6], Marta Álvarez[7], María F. Montero[8], Javier Arístegui[8]

Keywords: transparent exopolymer particles, prokaryotes, organic carbon, open ocean, Mediterranean Sea

[1] Departament de Biologia Marina i Oceanografia, Institut de Ciències del Mar, CSIC, Barcelona, Catalunya, Spain

[2] CNRS, Sorbonne Université, UMR 7621 Laboratoire d'Océanographie Microbienne, Observatoire Océanologique, Banyuls-sur-Mer, France

[3] Departamento de Ecología and Instituto del Agua, Universidad de Granada, Granada, Spain

[4] Research Unit "Modeling Nature" (MNat), Universidad de Granada, Granada, Spain

[5] Centre for Marine Ecosystems Research. School of Sciences, Edith Cowan University, Joondalup, WA, Australia

[6] Department of Oceanography, Instituto de Investigacións Mariñas, CSIC, Vigo, Spain

[7] Instituto Español de Oceanografía, Centro Oceanográfico de A Coruña, Spain

[8] Instituto de Oceanografía y Cambio Global, IOCAG, Universidad de Las Palmas de Gran Canaria, ULPGC, Las Palmas de Gran Canaria, Las Palmas, Spain

*corresponding author. E-mail: ortegartuerta@obs-banyuls.fr

Abstract

Transparent exopolymer particles (TEP) play a key role in ocean carbon export and structuring microbial habitats, but information on their distribution across different ocean basins and depths is scarce, particularly in the dark ocean. We measured TEP vertical distribution from the surface to bathypelagic waters in an east-to-west transect across the Mediterranean Sea (MedSea) and the adjacent North Eastern Atlantic Ocean (NEA), and explore their physical and biological drivers. TEP ranged from 0.6 to 81.7 µg XG eq L^{-1}, with the highest values in epipelagic waters above the deep chlorophyll maximum, and in areas near the Gibraltar and Sicily Straits. TEP were significantly related to particulate organic carbon (POC) in all basins and depth layers (epipelagic vs. deep), but the contribution of TEP to POC was higher in the NEA (85%, 79% and 67% in epi-, meso- and bathypelagic waters, respectively) than in the MedSea (from 53% to 62% in epipelagic waters, and from 45% to 48% in meso- and bathypelagic waters), coinciding with higher carbon to nitrogen particulate organic matter ratios in the NEA. The TEP connectivity between epipelagic waters and mesopelagic waters was less straightforward than between mesopelagic waters and bathypelagic waters, with a 23% and 55 % of the variance in the relationship between layers explained respectively. Prokaryotes were found to be a likely net source of TEP as inferred by the significant direct relationship observed between prokaryotic heterotrophic abundance and TEP. This assumption was confirmed using experimental incubations, where prokaryotes produced TEP in concentrations ranging from 0.7 (Western Mediterranean, bathypelagic) to 232 (Western Mediterranean, mesopelagic) µg XG eq. L^{-1} day^{-1}.

Keywords: transparent exopolymer particles, particulate organic carbon, prokaryotes, Mediterranean Sea, dark ocean, biological carbon pump

Introduction

Transparent Exopolymer particles (TEP) are polysaccharide-rich microgels (from ~0.4 to > 200 µm) with an ubiquitous distribution in the ocean, where they play a crucial role in transferring carbon from the dissolved to the particulate pool (Alldredge et al. 1993). On the one hand, TEP are sticky (Engel 2000; Passow and Alldredge 1995a), and can thus promote particle aggregation leading to their downward export when they are ballasted (Passow 2002b; Wurl et al. 2011), enhancing the biological carbon pump. On the other hand, these particles are porous and of low density and, consequently, may reduce the sinking rates of aggregates enriched in TEP. They can even float or ascend through the water column (Azetsu-Scott and Passow 2004; Mari et al. 2017), counteracting the downward export of particulate organic matter and affecting air-sea gas exchange after their accumulation in the surface microlayer (Wurl et al. 2011).

TEP net accumulation across marine environments is determined by the quality and quantity of the polymers released by microorganisms (Gogou and Repeta 2010), their degradation pathways (Taylor et al. 2014) and the environmental conditions promoting abiotic self-assembly of these polymers (Alldredge et al. 1993; Berman-Frank et al. 2016; Mari et al. 2005; Mopper et al. 1995). TEP were first described in cultures and natural proliferations of phytoplankton (Alldredge et al. 1993). Thenceforth, phytoplankton have been considered to be the main TEP source in the euphotic layer, also because high TEP concentrations have been regularly observed associated with phytoplankton blooms (Hong et al. 1997; Mari and Kiørboe 1996) and regions where algal biomass increased due to favourable growth conditions (Prieto et al. 2006). In contrast to highest TEP absolute values, relatively elevated TEP concentrations in relation to chlorophyll or primary production values may also be expected in oligotrophic areas since a high TEP formation per unit cell occurs under nutrient-depleted conditions and as a consequence of phytoplankton carbon overflow (Bar-Zeev et al., 2009; 2011).

In contrast to the unequivocal role of phytoplankton as a TEP source; the role of heterotrophic prokaryotes on TEP dynamics is less straightforward. Prokaryotes may act both as TEP sinks via colonization and degradation of the particles (Mari and Kiørboe 1996; Taylor et al. 2014) or as sources (Ortega-Retuerta et al. 2010; Passow 2002a), and interact with phytoplankton promoting TEP production (Gärdes et al. 2011; Gärdes et al. 2012). Heterotrophic prokaryotes release extracellular polymers during their growth, by producing mucous capsules (Decho 1990), or modifying the stickiness of the polymers (Rochelle-Newall et al. 2010; Van Oostende et al. 2013), contributing to the assembly of dissolved polymers into larger sized particles.

While all published studies to date have looked at TEP-prokaryote interactions in the euphotic layer or in laboratory experiments, there is no information on the role of heterotrophic prokaryotes on TEP formation in the dark ocean. In contrast to surface waters, the deep waters are enriched in inorganic nutrients and microbial metabolism is highly dependent on the downward flux of organic carbon from surface waters (Arístegui et al. 2009). Meso- and bathypelagic prokaryotes mostly sit on particles and are apparently well adapted to a particle-attached lifestyle (Baltar et al. 2009; Herndl and Reinthaler 2013). During sedimentation the particles evolve and it is well known that changes in

element stoichiometry (Engel et al. 2015; Radic et al. 2005) or the nature of the available organic matter (Koch et al. 2014; Ogawa et al. 2001) affect the prokaryotic production of TEP. Therefore, quantification of the net rates of TEP generation by prokaryotes in the deep ocean will help to better understand their contribution to the global carbon cycle and, principally, to particulate organic carbon (POC) flux attenuation.

The Mediterranean Sea is an oligotrophic ecosystem characterized by surface phosphorus limitation, particularly accentuated in the Levantine basin (Krom et al. 1991; Thingstad et al. 2005). This semi-enclosed sea is connected to the Northeast Atlantic Ocean through the highly dynamic and productive region of the Strait of Gibraltar, characterized by a two-layer system with an upper Atlantic layer inflowing into the Mediterranean Sea, and Mediterranean water outflowing at depth (Gascard and Richez 1985; Lacombe and Richez 1982). Frequent events of large mucus aggregates, preceded by periods with elevated TEP levels, have been observed in some regions of the Mediterranean Sea (i.e. coastal Adriatic and Aegean Seas, Radic et al., 2005; Danovaro et al., 2009). However, these local studies might not be representative of the entire basin and only a handful of studies have documented the variability of TEP concentrations in surface (Garcia et al., 2002; Ortega-Retuerta et al., 2010, 2016) and mesopelagic waters (Bar-Zeev et al., 2011; Prieto et al., 2006; Weinbauer et al., 2013), showing variable TEP accumulations both spatially and with depth.

Here we present a detailed and comprehensive vertical distribution of TEP across the Mediterranean Sea, from the eastern to the western basins, including the nearby Northeast Atlantic Ocean. We discuss TEP distribution in relation with water masses circulation and mixing, from the surface down to the dark sea, including for the first time the Mediterranean Sea bathypelagic waters. We also explore the different potential physical and biological factors that might drive TEP concentrations in the deep Mediterranean Sea, and quantify experimentally their production by heterotrophic prokaryotes.

2. Materials and Methods

2.1. Study site and sampling strategy

Sampling was carried out during the HOTMIX 2014 cruise on board the *R/V Sarmiento de Gamboa,* from 29th April to 28th May 2014. A total of 29 stations were sampled along a Mediterranean Sea section from East to West, also extending to the adjacent subtropical Northeast Atlantic Ocean (NEA) reaching the Canary Islands (Figure 1). Detailed information about the distributions of salinity, potential temperature and chlorophyll *a* concentrations as well as the water masses intercepted during the cruise is provided in Martínez-Pérez et al. (2017). Samples were collected using a rosette sampler holding 24 Niskin bottles (12 L each), coupled to a Seabird SBE 9-11 plus conductivity-temperature–pressure probe (CTD), complemented with a SBE43 oxygen sensor and a SeaTech fluorometer. Up to 13 depths were sampled covering the entire water column, from 3 m down to 10 m above the seafloor.

Samples from the epipelagic layer (surface water; down to 200 m) were systematically collected at four depths: 3 m, the depth receiving 20% of the surface photosynthetically active radiation, the depth of the deep chlorophyll maximum (DCM), and between 10 m and 45 m below the DCM. The depth of the DCM was determined after visual inspection of the vertical profiles of chlorophyll a (Chl *a*) fluorescence.

Sampling depths in the meso- and bathypelagic layers were decided on the basis of the full-depth potential temperature, salinity and dissolved oxygen profiles to ensure that all the water masses of the Mediterranean Sea and their respective mixing zones were sampled. More specifically, in the mesopelagic layer of the Eastern Mediterranean (EM) we focused our sampling efforts on the intermediate waters, including the Levantine Intermediate Water (LIW) and the Cretan Intermediate Water (CIW), which occupy the water column from 200 to 400 m depth. The core of the LIW can be easily characterised by its absolute salinity maximum. In the Western Mediterranean (WM), modified LIW and Winter Intermediate water (WIW) occupy the water column from 200 to 600 m depth. The modified LIW can be characterised not only by its salinity maximum but also by its absolute oxygen minimum. Finally, the bathypelagic layer is occupied by Eastern (EMDW) and Western (WMDW) Mediterranean Deep waters. Both the EMDW and WMDW are in fact composites of different varieties formed at different sites and/or under different conditions. In the Eastern Mediterranean, EMDW can be of Adriatic or Aegean origin and the waters of Adriatic origin form with different salinity and temperature depending on the climate conditions at the time of formation. The same is applicable to the WMDW where different varieties can be found depending on the proportions of Atlantic Water (AM) and/or LIW at the time of WMDW formation in the Gulf of Lions. In the North Eastern Atlantic NEA Ocean, we focused on three water masses and their mixing horizons: North Atlantic Central Water (NACW) between 200 to 750 m depth, Mediterranean Water (MW) from 750 to 1500 m depth, and North Atlantic Deep Water (NADW) from >1500 m. For a detailed description of the water masses during the cruise, see Catalá et al. (2018) (Supplementary Figure 1) for the Mediterranean water masses and Catalá et al. (2015) for the NEA water masses.

2.2. Analytical procedures

2.2.1. TEP

Transparent exopolymer particles (TEP) concentrations were measured using the colorimetric alcian blue method (Passow and Alldredge 1995b). Duplicate or triplicate samples (0.4 – 2 L) were filtered through 0.4 µm polycarbonate filters (25 mm diameter, Poretics) and the TEP retained on the filters were stained with 0.5 ml of a 0.02 % solution of alcian blue (Sigma) in 0.06 % acetic acid (pH 2.5). The stained filters were frozen at -80ºC until analysis in the laboratory (for less than 1 month). The alcian blue-stained TEP were extracted from the thawed filters adding 80 % sulphuric acid and the absorbance was measured at 787 nm in 1 cm path disposable polystyrene cuvettes using ultrapure water as blanks. Three blanks were performed for each batch of samples filtered every day (including staining and freezing in parallel to the samples). Each solution of alcian blue was calibrated using a fresh standard solution of xanthan gum. The coefficient of variation of the replicates was ~ 17 %. TEP concentration was expressed as micrograms of xanthan gum equivalents per liter (µg XG eq L^{-1}). To estimate TEP carbon content in our dataset, and with the aim of comparing with particulate organic carbon (POC) concentration, we used the canonical conversion factor of 0.75 µg C/ µg XG eq proposed in the literature (Engel and Passow 2001).

2.2.2. Particulate organic carbon (POC)

Samples for Particulate Organic Carbon (POC) were determined after filtering 2-4 L of the water samples through combusted (450ºC for 12 h) Whatman GF/F filters (25 mm diameter and 0.7µm nominal pore size). These filters were stored frozen (-20 ºC) until processed. In the laboratory, the filters were thawed and dried overnight at 65 ºC in a desiccator under HCl fumes to remove carbonates and, then, dried overnight in a desiccator with silica gel. The POC and PON analyses were performed by high-temperature (900 ºC) combustion in an elemental analyzer (Perkin Elmer 2400 CHN).

2.2.3. *Dissolved Oxygen (O_2), Inorganic Nitrogen (DIN) and Phosphorus (DIP)*

Samples for O_2 determination were collected in flared neck iodine calibrated flasks and measured using a Winkler potentiometric method adapted from Langdon (2010). Samples for inorganic nutrient analysis were collected in 50 mL polyethylene bottles and kept in the dark at 4 °C until analysis on board. Nitrate, phosphate and silicate concentrations were determined using a Skalar segmented flow autoanalyzer SAN++ following the colorimetric methods of Grasshoff et al. (1999).

2.2.4. Dissolved organic carbon (DOC)

DOC samples were filtered through pre-combusted (450ºC for 12 h) Whatman GF/F filters in an all-glass filtration system under positive pressure of high purity N_2 and collected into pre-combusted glass ampoules, acidified with phosphoric acid (final pH < 2), sealed and stored at 4ºC until analysis. Samples below 150 m were not filtered. These

samples were analyzed by high-temperature catalytic oxidation on a Shimadzu TOC-V total organic carbon analyzer. Potassium hydrogen phthalate (99.95–100.05%, p.a., Merck) was used to calibrate the system daily. The precision of the equipment was ±1 μmol L^{-1}. The accuracy was checked daily with the DOC reference materials provided by D. A. Hansell (University of Miami, USA).

2.2.5. Chlorophyll a (Chl a) concentration

For Chl-*a*, 500 mL of sea water were sampled and filtered through 25 mm Whatman GF/F filters under low vacuum pressure. The filters were kept frozen at -20ºC until analysis. Before chlorophyll a determination, pigments were extracted using 10 mL of 90% acetone at 4ºC in the dark for 24 h. Extracts were then measured fluorometrically, before and after acidification, by means of a Turner Designs bench fluorometer 10-AU, previously calibrated with pure chlorophyll a (Sigma Chemical), following Holm-Hansen et al. (1965).

2.2.6 Picophytoplankton abundance

Prochlorococcus and *Synechococcus* type cyanobacteria and small photosynthetic eukaryotic cells (picoeukaryotes) were enumerated with a FACScalibur (Becton and Dickinson) flow cytometer. Samples of about 1 mL were analyzed in fresh material 30-60 min after retrieval. Phytoplankton groups were identified by their signatures in a plot of side scatter (SSC) versus red (FL3) and orange (FL2) fluorescence. Samples were run at 60 mL min^{-1}. A suspension of yellow–green 1 μm latex beads (~10^5 beads mL^{-1}) was added as an internal standard (Polysciences, Inc.). Pigmented nanoeukaryotes (2-20 μm) were counted on fresh samples with a Cytobuoy cytometer (Dubelaar and Gerritzen 2000), provided with flow-imaging. Samples (about 3 ml) were analyzed *in vivo* for 7 min at a flow rate of 300 μL min^{-1}.

2.2.7. Prokaryotic heterotrophic abundance (PHA)

PHA was measured by flow cytometry (Gasol and del Giorgio, 2000). Aliquots of 1.5 mL were fixed with 2% of paraformaldehyde, deep-frozen in liquid nitrogen and then stored at -80 ºC until analysis, a few hours after collection. The samples were stained with SYBR Green I and run through a FACSCalibur cytometer fitted with a laser emitting at 488 nm. A suspension of yellow-green 1 μm latex beads was added as an internal standard (Polyscience Inc). The flow rate was determined volumetrically after every 10 samples.

2.2.8. Prokaryotic heterotrophic Production (PHP)

PHP rates were estimated from ^{3}H-Leucine (specific activities = 112 Ci $mmol^{-1}$) incorporation into proteins (Kirchman et al., 1985) and using the microcentrifugation protocol proposed by Smith and Azam (1992). Three replicates (1.2 ml) and two trichloroacetic acid (TCA)-killed blanks in microcentrifuge tubes were added L-[4, 5-^{3}H] leucine at 20 nM. Samples and blanks were incubated (for 3 to 15 h) at *in situ* temperatures. Incubations were stopped by adding 50% TCA. Subsequently, the samples were centrifuged twice (10 min. and 14000 r.p.m.) and rinsed with 5% TCA. Scintillation cocktail (1 mL Optisafe HiSafe) was added, and after 24 h, the samples were counted in a

liquid scintillation counter. Leucine incorporation rates (pmol Leu L^{-1} h^{-1}) were converted into carbon (µg C l^{-1} d^{-1}) by using a theoretical factor of 1.55 kg C mol Leu^{-1} (Simon and Azam, 1989), assuming negligible isotope dilution.

2.2.9. Optimum multiparameter (OMP) water mass analysis

Catalá et al. (2018) developed an OMP water mass analysis that allowed computing the contribution of the 19 deep water types identified during the HOTMIX 2014 cruise to every water sample (Supplementary Figure 1). The process included clustering the samples into mixing groups and creating an over-determined system of linear mixing equations for volume, potential temperature, salinity, NO (= O_2 + R_N · NO_3; with R_N = 9.4 mol O_2 mol N^{-1}) and silicate that was solved in a non–negative less–squares sense for each mixing group. In the Western Mediterranean, the shallowest mesopelagic water type considered was the Atlantic Water (AW) that enters the Mediterranean Sea across the Strait of Gibraltar. Below the AW the Winter Intermediate Water (WIW), formed in the slope of the Gulf of Lions and the Balearic Sea, and the Eastern Intermediate Water (EIW), which comes from the Eastern Mediterranean through the Strait of Sicily, were identified. The bathypelagic layer was occupied by five varieties of Western Mediterranean Deep Water (WMDW), formed in the Gulf of Lions. In the shallow Eastern Mediterranean, Modified Atlantic Water (MAW) in the Strait of Sicily and Levantine Surface Water (LSW) in the Levantine basin were the main water masses observed. The intermediate layer was occupied by the Levantine (LIW) and Cretan (CIW) intermediate waters. In the bathypelagic layer, five varieties of the Eastern Mediterranean Deep Water (EMDW) could be observed, one of Aegean origin (EMT) and four of Adriatic origin (Supplementary Figure 1).

2.2.10. Estimation of water mass archetype concentrations

Once the water mass proportions were calculated (see section 2.2.9), water-mass weighted average values of any variable N for each water mass (N_i), hereinafter "archetype values", were calculated as:

$$N_i = \frac{\sum_j x_{ij} \cdot N_j}{\sum_j x_{ij}}$$

where x_{ij} is the proportion of water mass i in sample j and N_j is the value of variable N in sample j. N_j is also called archetype value of N in water mass j, and retains the variability of N due to mixing and large scale biogeochemical processes from the formation area of the water mass to the study site (Álvarez-Salgado et al. 2013; Catalá et al. 2018).

The standard deviation of the archetype value of N for each water mass, SDN_i, was calculated as:

$$SDN_i = \frac{\sqrt{\sum_j x_{ij} \cdot (N_j - N_i)^2}}{\sum_j x_{ij}}$$

2.3. Prokaryotic TEP generation experiments

To quantify TEP formation by prokaryotes in the Mediterranean Sea, we performed a set of re-growth culture experiments using water from the well-contrasted Eastern and Western Mediterranean basins at different depths in a total of four incubations, two located in the Eastern basin and two located in the Western basin (Figure 1). Those using EIW were carried out in October 2013 during a previous test cruise between Barcelona and the island of Majorca. Water was incubated using triplicate 2 L Nalgene bottles, for 6 days, under *in situ* temperature conditions and in the dark. All used material was acid-washed and rinsed with ultrapure water prior to its use. The samples were pre-filtered through 1 µm filters (using 0.1N HCl pre-washed Preflow capsule filters, Pall Corporation), to remove large particles and grazers, and were used as inoculum of natural microbial populations. The water samples were subsequently filtered by 0.2 µm (using sterile Whatman Polycap cartridge filters). These fractions were mixed, and homogenized, with 75% of 0.2 µm filtered seawater + 25% of microbial inocula. Prokaryotic heterotrophic abundance (PHA) and production (PHP) were monitored during the course of the experiments (6 days) while the concentrations of TEP were determined at the onset and the end of the experiments.

2.4. Statistical Analyses

We used non-parametric Mann-Whitney U tests to compare differences in TEP and other variables among ocean basins. Depth-averaged data were calculated using the conventional trapezoid method. Linear regression analyses were used to investigate the decreases in TEP and POC concentration with depth, and reduced major axis (RMA) regressions were used to explore the environmental drivers of TEP variability in meso- and bathypelagic water masses, and the relationship between TEP increases and PHA and PHP increases along the incubations. All variables were $\log_{10}$ transformed prior to analyses to facilitate comparison between slopes. All these analyses were conducted using the lmodel2 package in the R software (Legendre 2014).

Results

3.1. Environmental conditions

Sea surface temperature ranged from 16.3ºC at station 17 (near the island of Corsica, Western Mediterranean basin) to 19.3 ºC at station 28 in the North Eastern Atlantic, and all visited stations were thermally stratified (Supplementary Figure 2A). Deep waters were increasingly warmer from West to East: waters >1000 m had on average 6.7 ± 4.4 ºC in the North Eastern Atlantic basin, 13.2 ± 0.6 ºC in the Western Mediterranean basin, and 14.0 ± 0.9 ºC in the Eastern Mediterranean basin (Supplementary Figure 2A). Salinity increased from West to East in all depth layers. A layer of high salinity (>39), indicative of the presence of LIW, was located in the Eastern Mediterranean basin from the surface to 400 m at station 1 (the Easternmost station) and became deeper (between 100 and 600 m) near the Sicily Strait, becoming mixed with other water masses in the Western Mediterranean basin (Supplementary Figure 2B). Salinity in the bathypelagic layer was on average 35.4 ± 0.45 at the North Eastern Atlantic, 38.5 ± 0.17 at the Western Mediterranean basin and 38.8 ± 0.45 at the Eastern Mediterranean basin (Supplementary Figure 2B).

The DCM was located deeper in the Eastern Mediterranean (up to 130 m) than in the Western Mediterranean (50-77m) and North Eastern Atlantic basin (60-86 m), according to the West to East increase in oligotrophy (Figure 2). The Chl *a* concentration in these maxima ranged from 0.13 (station 1, Eastern basin) to 0.92 µg L^{-1} (Station 23, Alboran Sea, Western Mediterranean basin). Particulate organic carbon (POC) concentrations ranged from 0.1 to 8.6 µmol L^{-1} (Supplementary Table 1) and significantly decreased with depth (log-log regression, $r^2 = 0.62$, p-value < 0.001; supplementary Figure 3). These decreases in POC; described with the slopes of the log-log regressions between depth and POC, were -0.33 (± 0.02) in the Eastern Mediterranean, -0.35 (± 0.02) in the Western Mediterranean and -0.31 (± 0.02) in the Northeastern Atlantic. The C:N ratios of particulate organic matter were significantly higher (Anova, $p < 0.005$) in the Atlantic Ocean than in both Mediterranean basins, particularly in the bathypelagic layer (supplementary Table 1)

3.2. TEP geographical distribution

TEP concentrations in the epipelagic layer increased from East to West (Table 1, Figure 2) and showed significant differences (Mann-Whitney U test) between all basins in the epipelagic layer ($p < 0.01$). In the meso- and bathypelagic layers, although TEP also increased from East to West (Table 1), the values were significantly higher in the North Atlantic Ocean ($p < 0.05$). However, although more TEP were observed in the Western than in the Eastern Mediterranean basins (Table 1), the differences were not significant. The highest TEP values were found at stations 22, 23 and 25, close to the Strait of Gibraltar in the upper 50 m (63.0 ± 7.0 µg XG eq L^{-1}), and the lowest TEP values (< 2 µg XG eq L^{-1}) were observed in the easternmost stations (station 1 between 500 and 1500 m, Figure 2). Significant and positive relationships were found between depth-averaged TEP concentrations in the mesopelagic and in the epipelagic layers (Figure 3A; slope= 0.78 ± 0.13, r^2= 0.23, $p<0.01$, n=29) and between depth-averaged TEP in the bathypelagic with

respect to that in the mesopelagic layer (Figure 3B; slope= 0.80 ± 0.11, r^2= 0.55, p<0.001, n=26), indicating a connection between layers. The explained variance for the mesopelagic-epipelagic relationship was lower than for the bathypelagic-mesopelagic relationship, suggesting that between the epipelagic and mesopelagic layers other pathways that release or remove TEP are affecting the distributions.

The TEP depth-profiles showed consistently higher concentrations in the epipelagic layer than in deeper waters (Figure 4). Within the epipelagic waters, TEP peaks were always shallower than the deep chlorophyll maxima, and were located at the surface in 13 out of 29 stations (located in the Levantine basin, the Ionic sea and the Gibraltar and Sicily straits) and between 40 and 50 m in 15 out of 29 stations (mainly in the Western Mediterranean and Eastern North Atlantic Ocean). TEP concentrations in the upper 200 m were maxima and ranged from 5.3 to 81.7 µg XG eq l^{-1}, with a median value of 30.9 µg XG eq L^{-1} (n = 121). By contrast, TEP concentrations in deep waters (≥ 200 m down to bottom depth) showed very constant values, with an average of 6.64 ± 0.02 µg XG eq L^{-1} (n = 221; Figure 4). Considering all data, the decline of TEP with depth could be described by the log-log regression Log_{10} TEP (µg XG eq L^{-1}) = -0.40 (± 0.03) Log_{10} depth (m) + 1.97 (± 0.09) (n = 342, r^2 = 0.60, p-value < 0.001). The slopes of the regression lines were different between the two Mediterranean basins and the adjacent Atlantic Ocean: The Atlantic slope (-0.33 ± 0.03) was significantly lower than those of the Mediterranean basins (-0.42 ± 0.02 and -0.40 ± 0.03 in the Eastern and Western Mediterranean respectively).

The TEP contribution to POC (expressed as a percentage) ranged from 3.3% to >100% and was higher in surface waters (up to 200 m depth) than in the meso- and bathypelagic waters (Table 1). This percentage was particularly high at the surface (3 m) and in subsurface waters (between 3 m and the DCM). Among basins, %POC values were consistently higher in the Northeast Atlantic than in the Mediterranean Sea (Table 1). However, no marked differences in these % were observed between meso- and bathypelagic waters (Table 1).

3.3. Environmental drivers of TEP distribution in the epipelagic and in the deep Mediterranean Sea

To test which were the main variables driving TEP distribution in the epipelagic and in the meso- and bathypelagic Mediterranean Sea, we used RMA regression analyses between TEP and a complex suite of environmental variables. TEP were not significantly related to Chl *a* concentration. However, we observed significant positive correlation between TEP and O_2 concentration, and between TEP and specific groups of phytoplankton (*Synechococcus*, pico- and nanophytoplankton, Table 2) and prokaryotic heterotrophic abundance (PHA) and production (PHP). Also negative relationships between dissolved inorganic nutrients and TEP were observed (Table 2). None of the correlations was particularly strong.

In the meso- and bathypelagic layers, RMA regressions showed significant relationships between the archetype TEP values in the water masses intercepted during the cruise (supplementary Figure 1) and archetype values of log-transformed temperature, dissolved organic carbon (DOC), particulate organic carbon (POC), and prokaryote

436 abundance (PHA) and production (PHP, Table 3). In addition, the regression equations
437 between archetypal temperature and TEP (Figure 5A) and between archetypal DOC and
438 TEP (Figure 5B) were significantly ($p < 0.01$) different between the Eastern and Western
439 basins (Table 3). In contrast, Archetypal TEP were also significantly and positively related
440 to archetypal POC (with $r^2 = 0.97$, Figure 5C) and archetypal prokaryotic abundance (PHA,
441 $r^2 = 0.94$, Figure 5D) and archetypal production (PHP, $r^2 = 0.76$, Table 3). In these analyses,
442 the intercepts and slopes of the regression equations were similar among basins (Table 3).
443 Comparing between layers, the POC-TEP relationships showed similar slopes in the
444 epipelagic and deep layers (Table 2, Table 3), while the in PHA-TEP relationships the slope
445 was significantly lower in the deep than in the epipelagic layer (Table 2, Table 3, Figure 6).
446
447 ***3.4. Prokaryotic TEP generation in experimental incubations***

448 Prokaryotic heterotrophic abundance (PHA) increased from 2 (Experiment with
449 WMDW) to 85-fold (EIW) during the incubations (Table 4). Prokaryotic heterotrophic
450 production (PHP) increased over time in all incubations and reached the plateau after three
451 days, with time- integrated PHP values of between 8.71 and 14.14 µg C L^{-1} for all the
452 experiments (Table 4). TEP concentrations increased in all incubations, with production
453 rates (ΔTEP) ranging from 0.7 (WMDW experiment) to 232.2 (EIW experiment) µg XG eq
454 L^{-1} d^{-1} (Table 4). The TEP production rates (ΔTEP) were significantly and positively related
455 to the increases in prokaryotic heterotrophic abundance ΔPHA ($r^2 = 0.99$, p-value < 0.007,
456 n = 4). The slope of the log-log regression equation between PHA and TEP observed in the
457 experiments (1.25 ± 0.09) was similar to that observed in situ in epipelagic waters (1.24 ±
458 0.19), but significantly higher than the one observed in deep waters (0.62 ± 0.04) (Figure
459 6).
460
461 **4. Discussion**
462
463 We present here the first basin-wide and full-depth dataset of TEP concentrations in
464 the open Mediterranean Sea. We observed consistent vertical profiles along the Eastern-
465 Western transect across the Mediterranean Sea and adjacent North Eastern Atlantic Ocean,
466 with higher TEP concentrations in the upper water column, being maximum above the
467 DCM depth, and lower and more uniform from 200 m down to the bottom (Figures 2 and
468 3). Stations close to the Straits of Gibraltar and Sicily exhibited the highest TEP
469 concentrations through the water column (68.4 and 69.8 µg XG eq L^{-1}, Figure 3). The range
470 of TEP concentrations observed in this study (0.6 - 81.7 µg XG eq L^{-1}) was comparable to
471 the values reported in some Mediterranean Sea regions (Table 5), such as the similar survey
472 carried out by Ortega-Retuerta et al. (2010) in epipelagic waters of the Mediterranean Sea,
473 in the region of the Strait of Gibraltar (Prieto et al. 2006), the Catalan Sea and Balearic Seas
474 (Iuculano et al. 2017; Ortega-Retuerta et al. 2018; Ortega-Retuerta et al. 2017) or the
475 Aegean Sea (Parinos et al. 2017). In other ocean areas, such as higher latitudes in the
476 Northeast Atlantic Ocean (Engel 2004; Harlay et al. 2010; Leblanc et al. 2009), the
477 oligotrophic western North Pacific Ocean (Kodama et al. 2014), or the Southern Ocean
478 (Ortega-Retuerta et al. 2009b) values within the range of the present study have also been
479 observed. In contrast, up to ten times higher epipelagic TEP concentrations were reported
480 in studies conducted in the waters of the Strait of Gibraltar (Prieto et al. 2006), and in the
481 ultraoligotrophic eastern Mediterranean basin (Bar-Zeev et al. 2011).

In deep waters, TEP concentrations were usually below 10 µg XG eq L^{-1}. There are only a handful of studies reporting TEP concentrations in the deep (> 200 m depth) Mediterranean Sea (Table 5): in the mesopelagic waters of the Strait of Gibraltar (Prieto et al. 2006), the Eastern Mediterranean (Bar-Zeev et al. 2011) and the Northwest Mediterranean (Ortega-Retuerta et al. 2017; Weinbauer et al. 2013). Only Bar-Zeev et al. (2011) observed higher (up to 80 times higher) values in the Eastern basin than the TEP range obtained in this study. The published information on TEP concentrations in other deep oceans basins is also scarce. Our concentrations are within the ranges of those published from the Pacific and Arctic Oceans by Wurl et al. (2011) but lower than those published by Yamada et al. (2017) from the Pacific Ocean and by Cisternas-Novoa et al. (2015) from the Sargasso Sea.

The TEP profiles in the surface waters of our study presented maximum values at depths located between the surface and the DCM. Previous studies in open waters have reported similar vertical profiles during the stratification period (Bar-Zeev et al. 2011; Kodama et al. 2014; Ortega-Retuerta et al. 2010; Ortega-Retuerta et al. 2017; Prieto et al. 2006; Wurl et al. 2011). These previous studies and our observations thus establish that this vertical pattern, with higher TEP concentrations in the epipelagic layer decreasing with depth, is very common at least during seasonal stratification, even at the beginning of the stratified season, when this study was carried out.

The significant relationships found between the depth-integrated TEP values in the epipelagic and the meso- and bathypelagic waters (Figure 4) suggest that the downward flux of particulate carbon, via TEP, into the deep waters must be important. Particularly robust were the relationships between meso- and bathypelagic layers, suggesting that the export of TEP from meso- to bathypelagic waters should be more efficient than that from epi- to mesopelagic waters. Another alternative explanation is that in the epipelagic layer there are TEP sinks that are absent or are relatively less important in deeper layers, such as photodegradation (Ortega-Retuerta et al. 2009a), emission to the atmosphere as primary aerosols (Orellana et al. 2011), or uptake and degradation by zooplankton (Ling and Alldredge 2003; Passow and Alldredge 1999; Taylor et al. 2014), which are more abundant and exhibit higher activity rates in epipelagic waters.

Noticeably, while the decrease in TEP with depth was similar in both Mediterranean Sea basins, it was lower in the Atlantic Ocean, as shown by a lower slope in the depth-TEP log-log relationship (Figure 2). This would suggest that, in the Atlantic Ocean, TEP is more efficiently transferred to deep waters than in the Mediterranean Sea. Although POC and TEP transfer efficiencies are still to be quantified by particle flux measurements, which were not performed in our study, this observation might help explain the relatively higher C:N molar ratios of particulate organic matter in the deep Atlantic basin (10.7 ± 2.0) than in the deep Mediterranean basin (9.1 ± 3.4 and 8.9 ± 0.8 in the Eastern and Western Mediterranean basins respectively, Supplementary Table 1), as TEP are known to be relatively enriched in carbon (Mari et al. 2001). The underlying reasons for this difference across oceans are yet unclear, but we could point to different non-exclusive mechanisms: Higher TEP uptake and TEP remineralization rates in the Mediterranean than in the

Atlantic would yield lower export efficiency. Although this fact is unknown for the TEP pool specifically, dissolved organic matter remineralization rates are higher in the deep Mediterranean Sea than in other ocean basins (Hansell et al. 2012; Santinelli et al. 2010), likely due to the about 10ºC higher temperature of the meso- and deep Mediterranean Sea waters compared with the world oceans. Also TEP production and cycling depends on the in situ microbial community composition (Engel et al. 2017) and environmental drivers such as nitrogen vs. phosphorus availability (Engel et al. 2015; Gärdes et al. 2012).

The percentage of POC that could be attributed to TEP in our study varied between 4 and >100% (Table 1) and was on average 75% of POC in the epipelagic Mediterranean Sea but 50% of POC in the deep Mediterranean layers. These values are in the upper range of previously published studies in the Atlantic Ocean (Engel 2004; Malpezzi et al. 2013), higher than in the West Coast of India (Bhaskar and Bhosle 2006), but lower than those measured in the Arctic Ocean (Yamada et al. 2015; Yamada et al. 2017), the Pacific Ocean (Yamada et al. 2017) or in the Eastern Mediterranean Sea (Bar-Zeev et al. 2011). Estimates of TEP contribution to the POC pool must be taken with caution, because in some of our samples the %TEP/POC was higher than 100%, a value impossible by definition, yet a fact that has been previously observed in Mediterranean Sea studies (Bar-Zeev et al. 2011; Parinos et al. 2017). The different cut-off filters used (GF/F for POC, 0.4 µm for TEP) make the comparisons difficult since small TEP are particularly abundant (Passow 2002b). In any case, the used invariant standard conversion factor from XG to TEP-C was calculated from phytoplankton cultures or waters enriched in phytoplankton (Engel and Passow 2001) but not present in our study. In situ TEP, particularly in the deep ocean, are likely derived from other sources, and their specific composition and properties, including their carbon content, is likely different than that in surface samples. Additional studies are definitely needed to obtain accurate estimations of TEP carbon content in contrasting locations and environmental scenarios, the deep ocean in our case.

Looking at the variability between ocean basins, the most remarkable feature is the higher contribution of TEP to the POC pool in the Atlantic Ocean: 79% in mesopelagic Atlantic waters opposed to 47% in mesopelagic Mediterranean Waters, and 67% in bathypelagic Atlantic waters, opposed to bathypelagic Mediterranean waters (48% and 45% in the E and W basins, Table 1). This difference likely reflects changes in POC export and the efficiency of the biological carbon pump between oceans. The decrease in TEP with depth was paralleled by the decrease in POC with depth: Both TEP and POC decreases with depth were lower in the Atlantic Ocean than in the Mediterranean Sea (supplementary Figure 1). This could be caused by the higher TEP contribution to POC in the Atlantic Ocean, that could enhance particle aggregation due to the high TEP stickiness (Logan et al. 1995).

In epipelagic waters, the uncoupling of Chl *a* and TEP distribution in our study was in line with previous observations in the Mediterranean Sea (Bar-Zeev et al. 2011; Ortega-Retuerta et al. 2010; Ortega-Retuerta et al. 2018; Ortega-Retuerta et al. 2017). This may reflect the inaccuracy of Chl *a* concentration as an estimator of phytoplankton biomass, as C:Chl *a* ratios vary in the water column due to e.g. photo-acclimation. In fact, we observed, that the highest TEP concentrations were generally shallower than the deep chlorophyll maxima, in agreement with Ortega-Retuerta et al. (2017). Moreover, the relatively good

relationship between TEP and O_2 suggests that primary production, not measured during the HOTMIX 2014 cruise, could be a better predictor of TEP distribution than Chl *a* in line with the results of Ortega-Retuerta et al. (2017). TEP distribution in the epipelagic was better predicted by the abundance of *Synechococcus*, micro- and nanoplankton. Although this is the first time a significant relationship between *Synechococcus* and TEP is shown, *Synechococcus* are known to produce aggregates (Deng et al. 2015). Conversely, prokaryotic abundance and production were related to TEP, as previously observed in the epipelagic Mediterranean Sea (Ortega-Retuerta et al. 2010). However, the relatively low explained variance in all these relationships illustrates the complexity of mechanisms driving TEP distributions and thus the difficulty in establishing a single predictor for TEP occurrence in the Mediterranean Sea.

The RMA regression analyses between archetype TEP and temperature or DOC showed different relationships between these variables in the two Mediterranean basins (Figure 5A-B, Table 3). In general, water masses from the Western Mediterranean were relatively more enriched in TEP compared to DOC than those from the Eastern basin. This observation supports the fact that a higher percentage of oxygen demand is due to DOC in the Eastern than in the Western basin (Catalá et. al. 2018). This difference in relative TEP concentrations (i.e. more TEP in water masses of similar temperatures) suggests that TEP in the Mediterranean Sea were not conservatively distributed with the different water masses (i.e. the main mechanisms transporting TEP to the ocean interior are not convection and/or deep water formation events).

Alternatively, the significant relationships between TEP and POC could be described using similar equations in the two Mediterranean basins (Figure 5C), so TEP could be similarly predicted by POC changes in both Mediterranean sub-basins. This suggests that TEP are distributed and cycled following pathways similar to those affecting bulk POC, i.e. particulate matter is mostly generated in surface layers and a fraction is exported downward to the deep Mediterranean Sea. This fraction is apparently similar for TEP and POC, as indicated by the similar slopes of POC-TEP relationships in epipelagic and deep waters (Table 2, Table 3). Our observations contrast with previous studies that show evidence of different export efficiencies of TEP and the overall POC pool in other ocean areas (Hamanaka et al. 2002; Mari et al. 2017).

TEP distribution in the meso- and bathypelagic waters are also well predicted by prokaryotic heterotrophic abundance (PHA, Table 3 and Figure 5D). Weinbauer et al. (2013) also observed significant relationships between heterotrophic prokaryotes and TEP concentrations in the twilight zone of the NW Mediterranean Sea, though not comparable to our study since they measured TEP microscopically. Although conditions for prokaryotes in the deep ocean are less favourable than in the epipelagic, and microbes grow at lower rates (Arístegui et al. 2009), deep ocean prokaryotes are also known to release gel-forming polysaccharides potentially generating TEP (Bar-Zeev et al. 2011).

The role of prokaryotes as a significant TEP source in the deep Mediterranean Sea was experimentally confirmed, as elevated amounts of TEP were generated following prokaryotic growth during all the incubations we performed, particularly in the mesopelagic waters assayed. This is, to our knowledge, the first experimental evidence of prokaryotic

622 TEP generation in deep ocean waters. Increases in TEP could be predicted from prokaryotic
623 growth, with rather similar per cell TEP generation rates in the four incubations. The
624 experimental generation rates presented similar slopes than the in situ PHA-TEP
625 relationship in epipelagic waters. Therefore, supporting previous evidences (Ortega-
626 Retuerta et al. 2010), we can conclude that TEP generation is the dominant process
627 determining the prokaryote-TEP relationship, so changes in prokaryote abundances would
628 be accompanied by similar changes in TEP as observed in the experiments. However, the
629 lower slope in the PHA-TEP relationship in the deep than in the epipelagic or in the
630 experiments suggests that prokaryotes in this layer do not only produce TEP but might also
631 consume and degrade TEP derived from other sources, likely those exported from the upper
632 layers. In this line, previous studies have shown intense prokaryote colonization of TEP in
633 the deep ocean (Bar-Zeev et al. 2011; Bochdansky et al. 2016).
634
635 **Conclusions**
636
637 We present the first basin-wide distribution of TEP in the Mediterranean Sea. We
638 conclude that TEP distribution and cycling patterns in the Mediterranean Sea are different
639 from those in the Atlantic Ocean, reflected in a more limited connectivity of TEP from the
640 epipelagic layer to the dark ocean -probably due to higher remineralization rates in the
641 Mediterranean Sea, but with higher TEP relative content in particles in the Atlantic Ocean.
642 This could translate into different POC export efficiencies among the different basins. In
643 situ measurements of particle fluxes in these ocean basins are needed to confirm this
644 hypothesis. Combining in situ data and experiments, we suggest that TEP sinking from
645 upper layers and in situ production by prokaryotes, mostly drive TEP spatial distribution in
646 Mediterranean meso- and bathypelagic layers.
647
648 **Acknowledgements**
649
650 This work was funded by project HOTMIX (CTM2011-30010/MAR) of the Spanish
651 Ministry of Economy and Innovation, co-financed with FEDER funds. Financial support
652 for the writing of this manuscript was also provided by project FLUXES (CTM2015-
653 69392-C3) to XAAS, MFM and JA, REMEI (CTM2015-70340-R) to JMG, and MNat
654 Scientific Unit of Excellence (UCE.PP2017.03) to IR. We would like to thank Nauzet
655 Hernández, Minerva Espino and Acorayda González (IOCAG, ULPGC) for their support at
656 sea, as well as in the laboratory analyses of PHA, POC and chlorophyll. The support of
657 María J. Pazó and Vanesa Vieitez (IIM, CSIC) analysing dissolved organic carbon and
658 inorganic nutrients is also acknowledged.
659
660
661 **References**
662
663 Alldredge, A.L., Passow, U., & Logan, B.E. (1993). The abundance and significance of a
664 class of large, transparent organic particles in the ocean. *Deep Sea Research I, 40*, 1131-
665 1140

666 Álvarez-Salgado, X.A., Nieto-Cid, M., Álvarez, M., Pérez, F.F., Morin, P., & Mercier, H.
667 (2013). New insights on the mineralization of dissolved organic matter in central,
668 intermediate, and deep water masses of the northeast North Atlantic. *Limnology and*
669 *Oceanography, 58*, 681-696

670 Arístegui, J., Gasol, J.M., Duarte, C.M., & Herndl, G.J. (2009). Microbial oceanography of
671 the dark ocean's pelagic realm. *Limnol Oceanogr, 54*, 1501-1529

672 Azetsu-Scott, K., & Passow, U. (2004). Ascending marine particles: Significance of
673 transparent exopolymer particles (TEP) in the upper ocean. *Limnology and Oceanography,*
674 *49*, 741-748

675 Baltar, F., Aristegui, J., Gasol, J.M., Sintes, E., van Aken, H.M., & Herndl, G.J. (2009).
676 High dissolved extracellular enzymatic activity in the deep central Atlantic Ocean. *Aquatic*
677 *Microbial Ecology, 58*, 287-302

678 Bar-Zeev, E., Berman, T., Rahav, E., Dishon, G., Herut, B., Kress, N., & Berman-Frank, I.
679 (2011). Transparent exopolymer particle (TEP) dynamics in the eastern Mediterranean Sea.
680 *Marine Ecology-Progress Series, 431*, 107-118

681 Berman-Frank, I., Spungin, D., Rahav, E., Van Wambeke, F., Turk-Kubo, K., & Moutin, T.
682 (2016). Dynamics of transparent exopolymer particles (TEP) during the VAHINE
683 mesocosm experiment in the New Caledonian lagoon. *Biogeosciences, 13*, 3793-3805

684 Bhaskar, P.V., & Bhosle, N.B. (2006). Dynamics of transparent exopolymeric particles
685 (TEP) and particle-associated carbohydrates in the Dona Paula bay, west coast of India.
686 *Journal of Earth System Science, 115*, 403-413

687 Bochdansky, A.B., Clouse, M.A., & Herndl, G.J. (2016). Dragon kings of the deep sea:
688 marine particles deviate markedly from the common number-size spectrum. *Sci Rep, 6*,
689 22633

690 Catalá, T.S., Martínez-Pérez, A.M., Nieto-Cid, M., Álvarez, M., Otero, J., Emelianov, M.,
691 Reche, I., Arístegui, J., & Álvarez-Salgado, X.A. (2018). Dissolved Organic Matter (DOM)
692 in the open Mediterranean Sea. I. Basin–wide distribution and drivers of chromophoric
693 DOM. *Progress in Oceanography, 165*, 35-51

694 Cisternas-Novoa, C., Lee, C., & Engel, A. (2015). Transparent exopolymer particles (TEP)
695 and Coomassie stainable particles (CSP): Differences between their origin and vertical
696 distributions in the ocean. *Marine Chemistry, 175*, 56-71

697 Decho, A.W. (1990). Microbial exopolymer secretions in ocean environments: their role (s)
698 in food webs and marine processes. *Oceanogr. Mar. Biol. Anny. Rev., 28*, 73-153

699 Deng, W., Monks, L., & Neuer, S. (2015). Effects of clay minerals on the aggregation and
700 subsequent settling of marineSynechococcus. *Limnology and Oceanography, 60*, 805-816

701 Dubelaar, G.B.J., & Gerritzen, P.L. (2000). CytoBuoy: a step forward towards using flow
702 cytometry in operational oceanography. *Sci Mar, 64*, 255-265

703 Engel, A. (2000). The role of transparent exopolymer particles (TEP) in the increase in
704 apparent particle stickiness (α) during the decline of a diatom bloom. *Journal of Plankton*
705 *Research, 22*, 485-497

706 Engel, A. (2004). Distribution of transparent exopolymer particles (TEP) in the northeast
707 Atlantic Ocean and their potential significance for aggregation processes. *Deep Sea*
708 *Research Part I: Oceanographic Research Papers, 51*, 83-92

709 Engel, A., Borchard, C., Loginova, A., Meyer, J., Hauss, H., & Kiko, R. (2015). Effects of
710 varied nitrate and phosphate supply on polysaccharidic and proteinaceous gel particle
711 production during tropical phytoplankton bloom experiments. *Biogeosciences, 12*, 5647-
712 5665

713 Engel, A., & Passow, U. (2001). Carbon and nitrogen content of transparent exopolymer
714 particles (TEP) in relation to their Alcian Blue adsorption. *Mar. Ecol. Prog Ser., 219*, 1-10

715 Engel, A., Piontek, J., Metfies, K., Endres, S., Sprong, P., Peeken, I., Gabler-Schwarz, S.,
716 & Nothig, E.M. (2017). Inter-annual variability of transparent exopolymer particles in the
717 Arctic Ocean reveals high sensitivity to ecosystem changes. *Sci Rep, 7*, 4129

718 Gärdes, A., Iversen, M.H., Grossart, H.P., Passow, U., & Ullrich, M.S. (2011). Diatom-
719 associated bacteria are required for aggregation of Thalassiosira weissflogii. *Isme Journal,*
720 *5*, 436-445

721 Gärdes, A., Ramaye, Y., Grossart, H.P., Passow, U., & Ullrich, M.S. (2012). Effects of
722 Marinobacter adhaerens HP15 on polymer exudation by Thalassiosira weissflogii at
723 different N:P ratios. *Marine Ecology Progress Series, 461*, 1-14

724 Gascard, J.C., & Richez, C. (1985). Water masses and circulation in the Western Alboran
725 sea and in the Straits of Gibraltar. *Progress in Oceanography, 15*, 157-216

726 Gogou, A., & Repeta, D.J. (2010). Particulate-dissolved transformations as a sink for semi-
727 labile dissolved organic matter: Chemical characterization of high molecular weight
728 dissolved and surface-active organic matter in seawater and in diatom cultures. *Marine*
729 *Chemistry, 121*, 215-223

730 Grasshoff, K., Kremling, K., & Ehrhardt, M. (1999). Determination of nutrients. In L.
731 Brügmann, & L. Kremling (Eds.), *Methods of Seawater Analysis*: WILEY–VCH Verlag

732 Hamanaka, J., Tanoue, E., Hama, T., & Handa, N. (2002). Production and export of
733 particulate fatty acids, carbohydrates and combined amino acids in the euphotic zone.
734 *Marine Chemistry, 77*, 55-69

735 Hansell, D.A., Carlson, C.A., & Schlitzer, R. (2012). Net removal of major marine
736 dissolved organic carbon fractions in the subsurface ocean. *Global Biogeochemical Cycles,*
737 *26*, n/a-n/a

738 Harlay, J., Borges, A.V., Van Der Zee, C., Delille, B., Godoi, R.H.M., Schiettecatte, L.S.,
739 Roevros, N., Aerts, K., Lapernat, P.E., Rebreanu, L., Groom, S., Daro, M.H., Van Grieken,
740 R., & Chou, L. (2010). Biogeochemical study of a coccolithophore bloom in the northern
741 Bay of Biscay (NE Atlantic Ocean) in June 2004. *Progress in Oceanography, 86*, 317-336

742 Herndl, G.J., & Reinthaler, T. (2013). Microbial control of the dark end of the biological
743 pump. *Nat Geosci, 6*, 718-724

744 Hong, Y., Smith Jr, W.O., & White, A.M. (1997). Studies on transparent exopolymer
745 particles (TEP) produced in the ross sea (Antarctica) and by Phaeocystis antarctica
746 (Prymnesiophyceae). *Journal of Phycology, 33*, 368-376

747 Iuculano, F., Duarte, C.M., Marbà, N., & Agustí, S. (2017). Seagrass as major source of
748 transparent exopolymer particles in the oligotrophic Mediterranean coast. *Biogeosciences,*
749 *14*, 5069-5075

750 Koch, B.P., Kattner, G., Witt, M., & Passow, U. (2014). Molecular insights into the
751 microbial formation of marine dissolved organic matter: recalcitrant or labile?
752 *Biogeosciences, 11*, 4173-4190

753 Kodama, T., Kurogi, H., Okazaki, M., Jinbo, T., Chow, S., Tomoda, T., Ichikawa, T., &
754 Watanabe, T. (2014). Vertical distribution of transparent exopolymer particle (TEP)
755 concentration in the oligotrophic western tropical North Pacific. *Marine Ecology Progress*
756 *Series, 513*, 29-37

757 Krom, M.D., Kress, N., & Brenner, S. (1991). Phosphorus limitation of primary
758 productivity in theeasternMediterranean Sea. *Limnol Oceanogr, 36*, 424-432

759 Lacombe, H., & Richez, C. (1982). The Regime of the Strait of Gibraltar. In J.C.J. Nihoul
760 (Ed.), *Elsevier Oceanography Series* (pp. 13-73): Elsevier

761 Langdon, C. (2010). Determination of dissolved oxygen in seawater by winkler titration
762 using the amperometric technique In ICPO (Ed.), *IOCCP Report No 14*

763 Leblanc, K., Hare, C.E., Feng, Y., Berg, G.M., DiTullio, G.R., Neeley, A., Benner, I.,
764 Sprengel, C., Beck, A., Sanudo-Wilhelmy, S.A., Passow, U., Klinck, K., Rowe, J.M.,
765 Wilhelm, S.W., Brown, C.W., & Hutchins, D.A. (2009). Distribution of calcifying and
766 silicifying phytoplankton in relation to environmental and biogeochemical parameters
767 during the late stages of the 2005 North East Atlantic Spring Bloom. *Biogeosciences, 6*,
768 2155-2179

769 Legendre, P. (2014). lmodel2: Model II Regression. R package version 1.7-2.
770 https://cran.r-project.org/package=lmodel2

771 Ling, S.C., & Alldredge, A.L. (2003). Does the marine copepod Calanus pacificus consume
772 transparent exopolymer particles (TEP)? *Journal of Plankton Research, 25*, 507-515

773 Logan, B.E., Passow, U., Alldredge, A.L., Grossartt, H.-P., & Simont, M. (1995). Rapid
774 formation and sedimentation of large aggregates is predictable from coagulation rates (half-
775 lives) of transparent exopolymer particles (TEP). *Deep Sea Research Part II: Topical*
776 *Studies in Oceanography, 42*, 203-214

777 Malpezzi, M.A., Sanford, L.P., & Crump, B.C. (2013). Abundance and distribution of
778 transparent exopolymer particles in the estuarine turbidity maximum of Chesapeake Bay.
779 *Marine Ecology Progress Series, 486*, 23-35

780 Mari, X., Beauvais, S., Lemée, R., & Pedrotti, M.L. (2001). Non-Redfield C : N ratio of
781 transparent exopolymeric particles in the northwestern Mediterranean Sea. *Limnology and*
782 *Oceanography, 46*, 1831-1836

783 Mari, X., & Kiørboe, T. (1996). Abundance, size distribution and bacterial colonization of
784 transparent exopolymeric particles (TEP) during spring in the Kattegat. *Journal of Plankton*
785 *Research, 18*, 969-986

786 Mari, X., Passow, U., Migon, C., Burd, A.B., & Legendre, L. (2017). Transparent
787 exopolymer particles: Effects on carbon cycling in the ocean. *Progress in Oceanography,*
788 *151*, 13-37

789 Mari, X., Rassoulzadegan, F., Brussaard, C.P.D., & Wassmann, P. (2005). Dynamics of
790 transparent exopolymeric particles (TEP) production by Phaeocystis globosa under N- or P-
791 limitation: a controlling factor of the retention/export balance. *Harmful Algae, 4*, 895-914

792 Martínez-Pérez, A.M., Osterholz, H., Nieto-Cid, M., Álvarez, M., Dittmar, T., & Álvarez-
793 Salgado, X.A. (2017). Molecular composition of dissolved organic matter in the
794 Mediterranean Sea. *Limnology and Oceanography, 62*, 2699-2712

795 Mopper, K., zhou, J., Sri Ramana, K., passow, U., dam, H.G., & Drapeau, D.T. (1995). The
796 role of surface-active carbohydrates in the flocculation of a diatom bloom in a mesocosm.
797 *Deep Sea Research Part II: Topical Studies in Oceanography, 42*, 47-73

798 Ogawa, H., Amagai, Y., Koike, I., Kaiser, K., & Benner, R. (2001). Production of
799 Refractory Dissolved Organic Matter by Bacteria. *Science, 292*, 917-920

800 Orellana, M.V., Matrai, P.A., Leck, C., Rauschenberg, C.D., Lee, A.M., & Coz, E. (2011).
801 Marine microgels as a source of cloud condensation nuclei in the high Arctic. *Proceedings*
802 *of the National Academy of Sciences, 108*, 13612-13617

803 Ortega-Retuerta, E., Duarte, C.M., & Reche, I. (2010). Significance of Bacterial Activity
804 for the Distribution and Dynamics of Transparent Exopolymer Particles in the
805 Mediterranean Sea. *Microbial Ecology, 59*, 808-818

806 Ortega-Retuerta, E., Marrasé, C., Muñoz-Fernández, A., Sala, M.M., Simó, R., & Gasol,
807 J.M. (2018). Seasonal dynamics of transparent exopolymer particles (TEP) and their drivers
808 in the coastal NW Mediterranean Sea. *Science of the Total Environment, 631*, 180-190

809 Ortega-Retuerta, E., Passow, U., Duarte, C.M., & Reche, I. (2009a). Effects of ultraviolet B
810 radiation on (not so) transparent exopolymer particles. *Biogeosciences, 6*, 3071-3080

811 Ortega-Retuerta, E., Reche, I., Pulido-Villena, E., Agustí, S., & Duarte, C.M. (2009b).
812 Uncoupled distributions of transparent exopolymer particles (TEP) and dissolved
813 carbohydrates in the Southern Ocean. *Marine Chemistry, 115*, 59-65

814 Ortega-Retuerta, E., Sala, M.M., Mestre, M., Borrull, E., Marrasé, C., Aparicio, F.L.,
815 Gallisai, R., Antequera, C., Peters, F., Simó, R., & Gasol, J.M. (2017). Horizontal and
816 vertical distributions of Transparent exopolymer particles (TEP) in the NW Mediterranean
817 Sea are linked to chlorophyll a and O2 variability. *Frontiers in Microbiology, 7*, 2159

818 Parinos, C., Gogou, A., Krasakopoulou, E., Lagaria, A., Giannakourou, A., Karageorgis,
819 A.P., & Psarra, S. (2017). Transparent Exopolymer Particles (TEP) in the NE Aegean Sea
820 frontal area: Seasonal dynamics under the influence of Black Sea water. *Continental Shelf*
821 *Research, 149*, 112-123

822 Passow, U. (2002a). Production of transparent exopolymer particles (TEP) by phyto- and
823 bacterioplankton. *Marine Ecology Progress Series, 236*, 1-12

824 Passow, U. (2002b). Transparent exopolymer particles (TEP) in aquatic environments.
825 *Progress in Oceanography, 55*, 287-333

826 Passow, U., & Alldredge, A.L. (1995a). Aggregation of a diatom bloom in a mesocosm:
827 The role of transparent exopolymer particles (TEP). *Deep-Sea Research Part II, 42*, 99-109

828 Passow, U., & Alldredge, A.L. (1995b). A dye-binding assay for the spectrophotometric
829 measurement of transparent exopolymer particles (TEP). *Limnology and Oceanography,*
830 *40*, 1326-1335

831 Passow, U., & Alldredge, A.L. (1999). Do transparent exopolymer particles (TEP) inhibit
832 grazing by the euphausiid Euphausia pacifica? *Journal of Plankton Research, 21*, 2203-
833 2217

834 Prieto, L., Navarro, G., Cózar, A., Echevarría, F., & García, C.M. (2006). Distribution of
835 TEP in the euphotic and upper mesopelagic zones of the southern Iberian coasts. *Deep Sea*
836 *Research Part II: Topical Studies in Oceanography, 53*, 1314-1328

837 Radic, T., Kraus, R., Fuks, D., Radic, J., & Pecar, O. (2005). Transparent exopolymeric
838 particles' distribution in the northern Adriatic and their relation to microphytoplankton
839 biomass and composition. *Science of the Total Environment, 353*, 151-161

840 Rochelle-Newall, E.J., Mari, X., & Pringault, O. (2010). Sticking properties of transparent
841 exopolymeric particles (TEP) during aging and biodegradation. *Journal of Plankton*
842 *Research, 32*, 1433-1442

Santinelli, C., Nannicini, L., & Seritti, A. (2010). DOC dynamics in the meso and bathypelagic layers of the Mediterranean Sea. *Deep Sea Research Part II: Topical Studies in Oceanography, 57*, 1446-1459

Taylor, J.D., Cottingham, S.D., Billinge, J., & Cunliffe, M. (2014). Seasonal microbial community dynamics correlate with phytoplankton-derived polysaccharides in surface coastal waters. *ISME J, 8*, 245-248

Thingstad, T., Krom, M.D., Mantoura, F., Flaten, G., Groom, S., Herut, B., Kress, N., Law, C.S., Pasternak, A., Pitta, P., Psarra, S., Rassoulzadegan, F., Tanaka, T., Tselepides, A., Wassmann, P., Woodward, M., Riser, C., Zodiatis, G., & Zohary, T. (2005). Nature of phosphorus limitation in the ultraoligotrophic eastern mediterranean. *Science, 309*, 1068-1071

Van Oostende, N., Moerdijk-Poortvliet, T.C., Boschker, H.T., Vyverman, W., & Sabbe, K. (2013). Release of dissolved carbohydrates by Emiliania huxleyi and formation of transparent exopolymer particles depend on algal life cycle and bacterial activity. *Environ Microbiol, 15*, 1514-1531

Weinbauer, M.G., Liu, J., Motegi, C., Maier, C., Pedrotti, M.L., Dai, M., & Gattuso, J.P. (2013). Seasonal variability of microbial respiration and bacterial and archaeal community composition in the upper twilight zone. *Aquatic Microbial Ecology, 71*, 99-115

Wurl, O., Miller, L., & Vagle, S. (2011). Production and fate of transparent exopolymer particles in the ocean. *Journal of Geophysical Research-Oceans, 116*

Yamada, Y., Fukuda, H., Uchimiya, M., Motegi, C., Nishino, S., Kikuchi, T., & Nagata, T. (2015). Localized accumulation and a shelf-basin gradient of particles in the Chukchi Sea and Canada Basin, western Arctic. *Journal of Geophysical Research: Oceans, 120*, 4638-4653

Yamada, Y., Yokokawa, T., Uchimiya, M., Nishino, S., Fukuda, H., Ogawa, H., & Nagata, T. (2017). Transparent exopolymer particles (TEP) in the deep ocean: full-depth distribution patterns and contribution to the organic carbon pool. *Marine Ecology Progress Series, 583*, 81-93

Figure 1. Map showing the sampling stations (numbers from 1 to 29) during the HOTMIX 2014 cruise. The strait of Sicily separates the Eastern (stations 1 to 13) from the Western (stations 14 to 15) basins; while the strait of Gibraltar separates the Mediterranean Sea from the subtropical Northeast Atlantic Ocean (stations 25 to 29). Yellow dots represent the locations where the experimental incubations were performed (EM LIW: Eastern Mediterranean Levantine Intermediate Water. EM DCM: Eastern Mediterranean deep chlorophyll maximum water. EIW: Western Mediterranean Levantine Intermediate Water. WM DW: Western Mediterranean Deep Water. This last experiment was performed in October 2013 during a previous test cruise between Barcelona and the island of Majorca

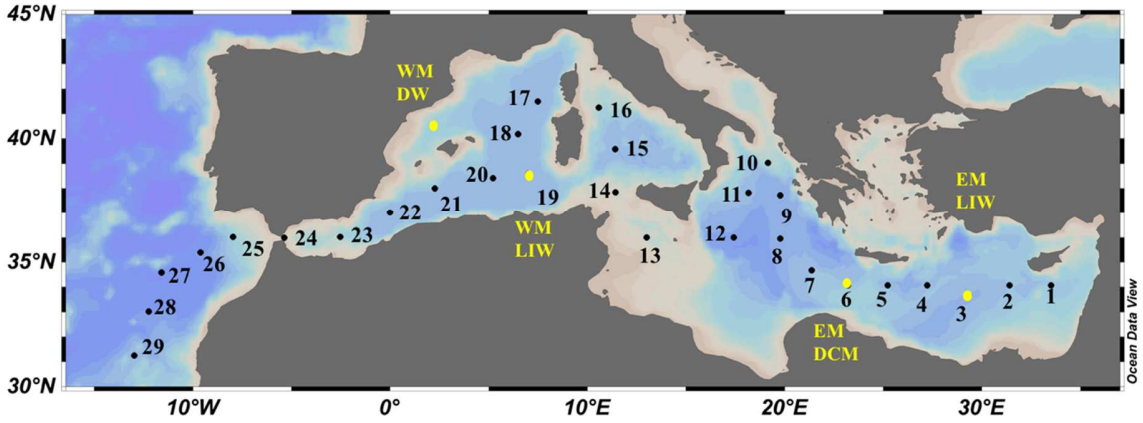

Figure 2. Distribution of transparent exopolymeric particles (TEP) during the HOTMIX 2014 cruise across the Mediterranean Sea and the Northeast Atlantic Ocean. White dashed lines indicate the approximate boundaries between ocean basins. Black dots correspond to the sampled stations and depths. The continuous white line in the upper panel indicates the depth of the deep chlorophyll maximum.

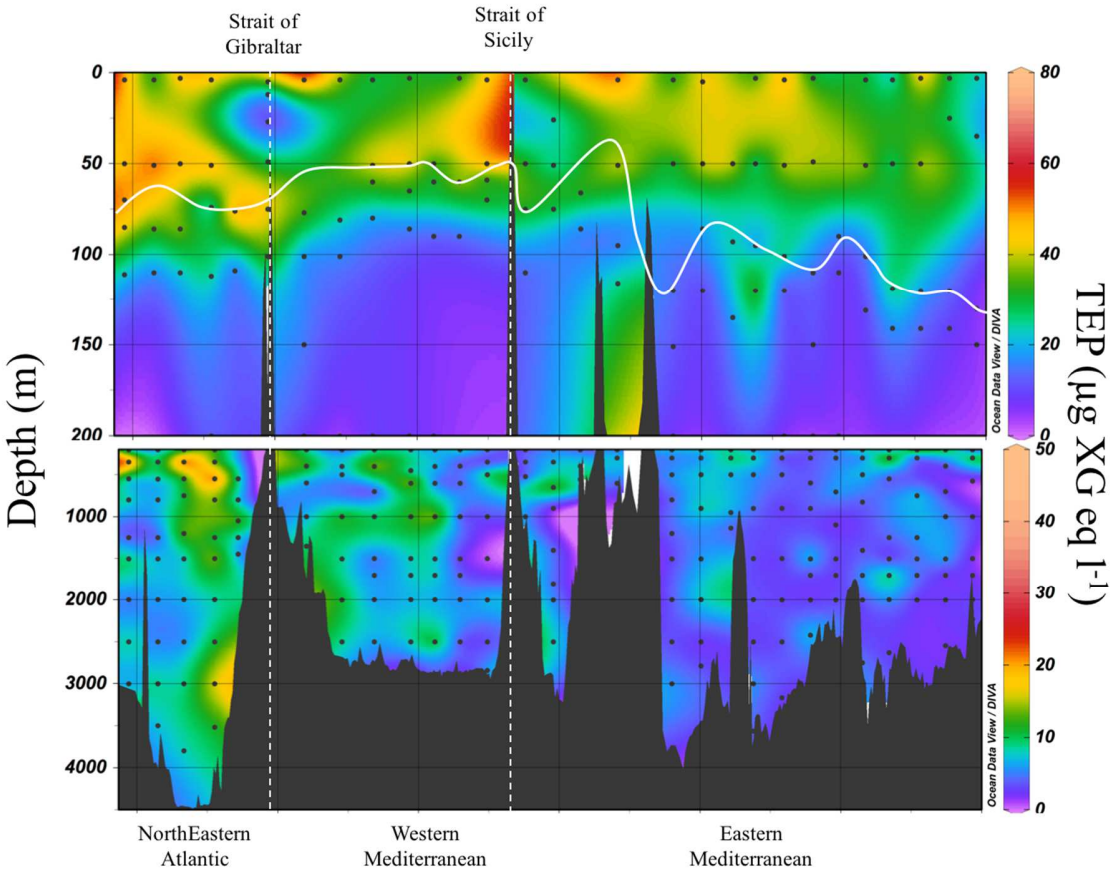

Figure 3. Scatter plots showing RMA regressions between depth-integrated transparent exopolymer particles (TEP) concentration in mesopelagic vs. epipelagic waters (a) and in bathypelagic vs. mesopelagic waters (b). The slopes of the regression lines are 0.78 ± 0.13 for the epi-meso relationship and 0.80 ± 0.11 for the meso-bathy relationship. (EM: Eastern Mediterranean, green triangles. WM: Western Mediterranean, black squares. NEA: Northeastern Atlantic Ocean, light blue circles)

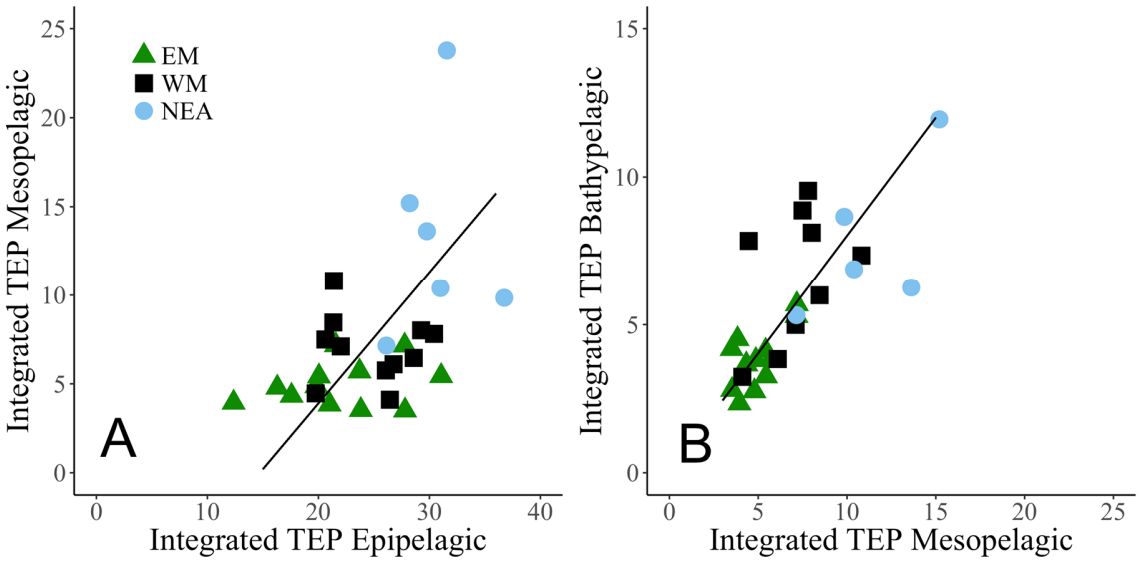

Figure 4. Depth profiles of transparent exopolymer particle (TEP) concentration in the three ocean basins sampled in this study. Horizontal dashed lines at 200 m and 1000 m separate the three depth layers (epipelagic, mesopelagic, bathypelagic). The different symbols discriminate between ocean basins (EM: Eastern Mediterranean, green triangles. WM: Western Mediterranean, black squares. NEA: Northeastern Atlantic Ocean, light blue circles)

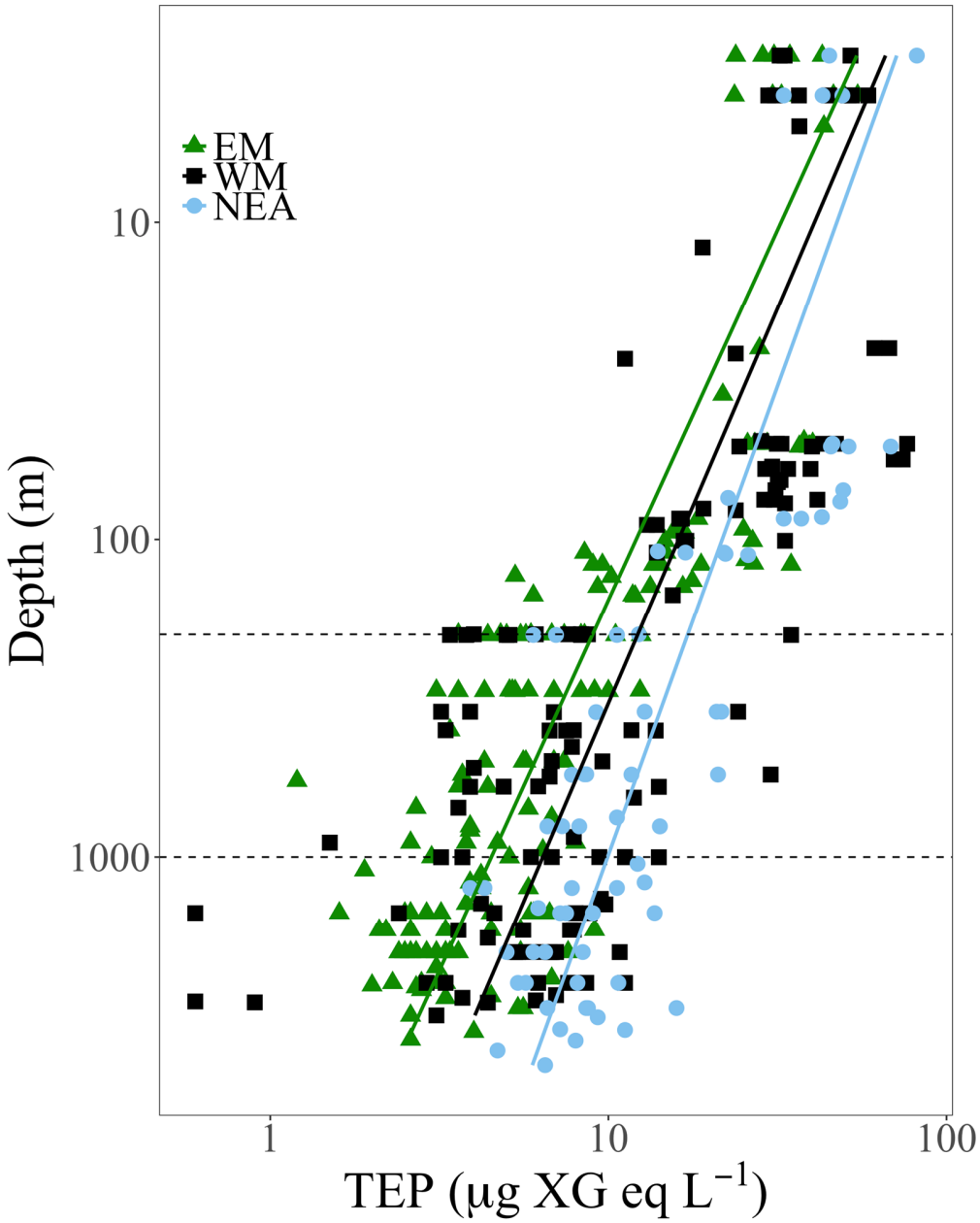

Figure 5. Scatter plots showing log-log RMA regression analyses between archetype values of temperature (TPot, A), dissolved organic carbon (DOC, B), particulate organic carbon (POC, C), and prokaryotic heterotrophic abundance (PHA, D), and archetype TEP concentrations in the meso- and bathypelagic water masses of the Mediterranean Sea. The regression equations are presented in Table 3. Green triangles: Eastern Mediterranean basin. Light blue squares: Western Mediterranean basin.

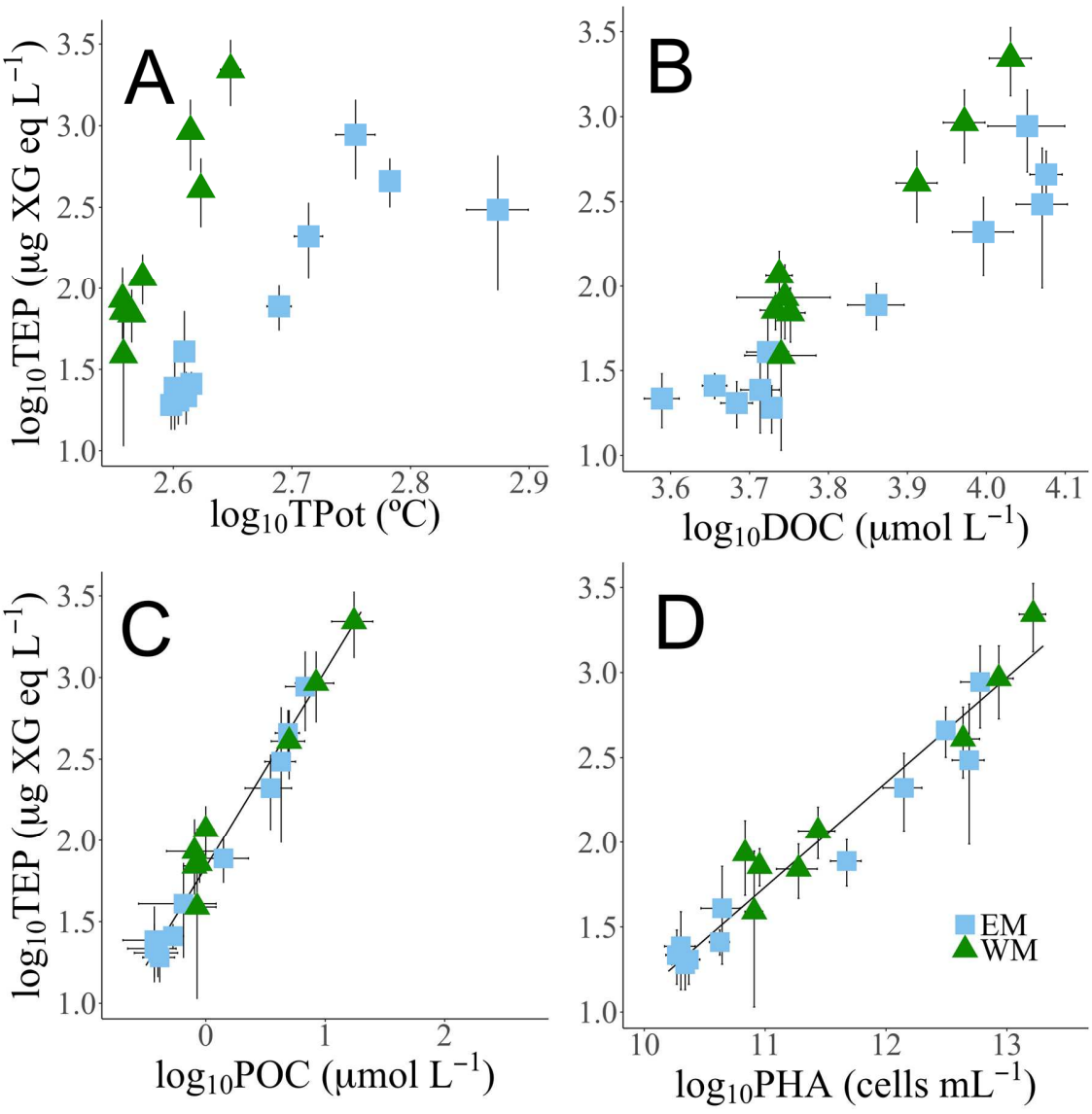

Figure 6. Log-log RMA relationships between prokaryotic heterotrophic abundance (PHA) and transparent exopolymer particles (TEP) in epipelagic waters (Epi, open green circles), and deep waters (Deep, dark blue diamonds) and between daily increases in PHA (ΔPHA) and increases in TEP (ΔTEP) in the experimental incubations (Exp, red triangles).

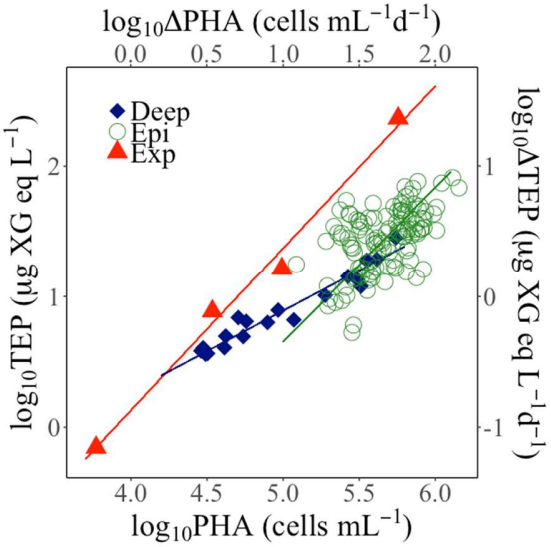

Table 1. Average (± Standard Error) and ranges (in brackets) of TEP concentrations (µg XG eq l^{-1}) and the fraction of TEP as particulate organic carbon pool (%POC) for each depth layer (epi-, meso and bathypelagic waters) in the different ocean basins. We used a constant conversion factor of 0.75 µgC µgXG eq^{-1} taken from the literature (Engel and Passow 2001).

Basin	Variable	Epipelagic	Mesopelagic	Bathypelagic
Eastern Med	TEP	25.1 ± 0.25 (5.3-54.6)	5.7 ± 0.05 (1.2-12.5)	3.8 ± 0.03 (1.6-9.1)
Western Med		34.8 ± 0.34 (11.2-76.5)	8.6 ± 0.16 (1.5-34.7)	5.9 ± 0.08 (0.6-11.2)
NE Atlantic		40.2 ± 0.79 (14.0-81.7)	11.4 ± 0.28 (6.0-21.6)	8.2 ± 0.10 (3.9-15.9)
Eastern Med	%POC	62.0 ± 0.5 (14.8-144.8)	47.2 ± 0.6 (8.6-157.9)	47.5 ± 0.8 (8.6-256.4)
Western Med		53.1 ± 0.5 (19.5-147.1)	46.9 ± 0.8 (12.9-197.6)	44.7 ± 0.8 (3.3-137.7)
NE Atlantic		85.2 ± 1.6 (27.2-139.2)	78.7 ± 3.0 (33.5-182.8)	66.7 ± 1.2 (22.1-169.1)

Table 2. Results of log-log RMA regression analysis between temperature (Temp), salinity (Sal), dissolved inorganic phosphorus (DIP) and nitrogen (DIN), particulate organic carbon (POC), abundances of different phytoplankton groups, dissolved oxygen concentration (O_2) prokaryotic heterotrophic abundance (PHA) and production (PHP) as independent variables and TEP (independent variable) in epipelagic waters along the HOTMIX 2014 cruise. r^2= explained variance; p= level of significance

Dep.Var	Independent Var.	Intercept	slope	r^2	p	n
TEP	Temp	-3.88 ± 2.89	2.57 ± 0.03	0.06	0.009	119
	Sal	50.25 ± 10.14	-12.91 ± 0.06	0.16	< 0.001	119
	DIP	1.91 ± 0.27	-0.31 ± 0.06	0.22	< 0.001	114
	DIN	2.93 ± 0.06	-0.20 ± 0.04	0.25	< 0.001	108
	POC	1.81 ± 0.19	1.36 ± 0.17	0.38	< 0.001	116
	Chl *a*				ns	
	Prochlorococcus				ns	
	Synechococcus	0.73 ± 0.32	0.30 ± 0.05	0.26	< 0.001	118
	Picophytoplankton	-4.01 ± 1.97	0.98 ± 0.26	0.14	< 0.001	119
	Nanophytoplankton	1.15 ± 0.33	0.49 ± 0.08	0.29	< 0.001	119
	Microphytoplankton	1.61 ± 0.64	0.49 ± 0.19	0.08	0.002	119
	Cryptophytes				ns	
	O_2	-60.59 ± 9.42	11.76 ± 1.73	0.31	< 0.001	119
	PHA	-12.82 ± 2.50	1.24 ± 0.19	0.28	< 0.001	119
	PHP	4.46 ± 0.30	0.62 ± 0.17	0.14	< 0.001	114

Table 3. Results of log-log RMA regression analyses between archetype values of temperature (temp), dissolved organic carbon (DOC), particulate organic carbon (POC), heterotrophic prokaryotic abundance (PHA) and prokaryotic heterotrophic production (PHP) and archetype values of transparent exopolymer particles (TEP) in meso- and bathypelagic waters of the Mediterranean Sea, both merged and split into Eastern and Western basins. r^2= explained variance; p= level of significance

Dep. Var.	**Ind. Var**	**All basins (n=19)**				**Eastern basin (n=11)**				**Western basin (n=8)**			
		r^2	p	Intercept ±SE	Slope ±SE	r^2	p	Intercept ±SE	Slope ±SE	r^2	p	Intercept ±SE	Slope ±SE
TEP	Temp	0.25	0.03	-19.96 ±17.65	8.33 ±6.69	0.78	<0.001	-16.07 ±3.98	6.70 ±1.49	0.93	<0.001	-42.45 ±6.60	17.28 ±2.56
"	DOC	0.79	<0.001	-13.31 ±2.10	4.01 ±0.55	0.91	<0.001	-10.93 ±1.55	3.34 ±0.41	0.95	<0.001	-17.00 ±4.89	5.04 ±0.61
"	POC	0.97	<0.001	1.84 ±0.01	1.21 ±0.06	0.98	<0.001	1.79 ±0.01	1.21 ±0.07	0.96	<0.001	1.91 ±0.04	1.14 ±0.12
"	PHA	0.94	<0.001	-5.05 ±0.46	0.62 ±0.04	0.96	<0.001	-4.72 ±0.55	0.58 ±0.05	0.94	<0.001	-5.12 ±1.01	0.63 ±0.08
"	PHP	0.76	<0.001	4.15 ±1.26	0.77 ±0.12	0.80	<0.001	4.43 ±0.52	0.90 ±0.19	0.78	0.004	3.85 ±0.49	0.62 ±0.19

Table 4. Average, and standard deviation (in brackets), of the daily increments in prokaryotic heterotrophic abundance (ΔPHA), time-integrated prokaryotic heterotrophic production (PHP), the average bacterial specific growth rates (SGR) and the daily TEP generation rates (ΔTEP).

Experiment	**ΔPHA (x 10^7 cells L^{-1} d^{-1})**	**PHP_{int} (µg C L^{-1})**	**SGR (d^{-1})**	**ΔTEP (µg XG eq L^{-1} d^{-1})**
Western Mediterranean *-Deep water*	0.59 (± 0.07)	-	0.13	0.7 (± 0.1)
Western Mediterranean *-Levantine intermediate water*	57.05 (± 0.25)	14.14	0.71	232.2 (± 14.6)
Eastern Mediterranean *-DCM water*	3.43 (± 0.26)	8.97	0.17	7.7 (± 3.0)
Eastern Mediterranean *-Levantine intermediate water*	9.81 (± 0.71)	8.71	0.69	16.4 (± 5.0)

Table 5. TEP concentrations in the Mediterranean Sea published in the literature.

Region	Depth (m)	Month	Year	TEP (µg XG eq l^{-1})	Chl (µg l^{-1})	POC (µmol l^{-1})	Ref
Levantine basin	surface	March/Jul/Sep	2008/2009	116-420	0.04-0.07	13.8	(Bar-Zeev et al. 2011)
"	dcm		"	48-189	<0.32		"
"	>300		"	83-386			"
North Western	4-200	May-June	2012	4.9-54.2	0.10-0.65	3.7-7.2	(Ortega-Retuerta et al. 2017)
"	200-2300	May-June	2012	5.2-19.0			"
North Western	surface	3 years	2012-2014	11.3-289.1	0.15-1.21	5.4-24.0	(Ortega-Retuerta et al. 2018)
Coastal NW (rocky shore)	surface	3 years	2012-2015	4.6-90.6	0.02-0. 54		(Iuculano et al. 2017)
Coastal NW (seagrass litter)	surface	3 years	2012-2015	26.8-1878.4	0.02-0. 54		"
North Western	20-50 (dcm)	1 year	1999-2000	0.35-.2 x10^7 *	<2.9	3.70-10.35	(Beauvais et al. 2003)
North Western	300m	1 year	2008-2009	0.52-1.4 x10^6 *			(Weinbauer et al. 2013)
Alboran Sea Inshore	0-70	June-July	1997	507-560			(Prieto et al. 2006)
Alboran Sea offshore	"		"	25-121			"
East-West transect	0-200	May	2007	4.5-94.3	0-1.78		(Ortega-Retuerta et al. 2010)
Aegean Sea	0-100	October	"	15.4-81.4	0.08-0.30	2.15-5.84	(Parinos et al. 2017)
"	"	March	"	39.1-188	0.04-0.60	1.64-9.75	
"	"	July	"	31.7-156	0.04-0.50	2.01-7.00	
Coastal Aegean	0-5	June-Jul/Jan-Feb	2003-2004	208-441	0.5-1.6	0.28-1.28	(Scoullos et al. 2006)
Coastal Adriatic	0- 37	1 year	1999-2002	4-14800	>1		(Radic et al. 2005)
East-West transect	0-200	May	2014	5.6-76.5	0.13-0.92	0.10-8.60	This study
"	201-1000	May	2014	1.2-34.7		0.26-5.37	"
"	1001-bottom	May	2014	0.6-11.2		0.13-1.62	"

* TEP analysed by microscopy counting